Microzoning of site response parameters in the towns of Dimona and Bet Shean (Israel)

Y. Zaslavsky[1], G. Ataev[1], M. Gorstein[1], M. Kalmanovich[1], A. Hofstetter[1], N. Perelman[1], T. Aksinenko[1], V. Giller[1], H. Dan[1], D. Giller[1], I. Livshits[1], A. Shvartsburg[1] and A. Shapira[2].

[1]*Seismology Division, Geophysical Institute of Israel, Israel*
[2]*International Seismological Centre, Thatcham, Berkshire, UK*

(Received: January 25, 2007; accepted: October 1, 2007)

ABSTRACT Due to their proximity to the seismically active Dead Sea Fault system, the towns of Dimona and Bet Shean are considered high seismic risk zones. An investigation of the possible site amplification effects, using ambient noise surveys, was carried out at 275 sites in Dimona and 210 sites in Bet Shean. The soil sites exhibit H/V peak amplitudes ranging from 2 to 7 in the frequency range 1.0 Hz to 10 Hz. While integrating data from the extensive ambient noise measurements, information about the regional geology and S-wave velocity profiles derived from a few refraction lines enabled the construction of multi-layer soil-column models that yield analytical site response functions which are consistent with the observed H/V spectral ratios. We divided the study areas into zones and characterized each of them with a generalized soil column model. Thus the seismic hazard zonation maps obtained are closely tied to site effects actually measured, and therefore may lead to realistic site-specific seismic hazard assessments in these towns, in spite of the paucity of borehole, refraction data and other subsurface information.

1. Introduction

The towns of Dimona and Bet Shean are situated along the seismically active Dead Sea Fault (DSF) system. Deformation of young sediments, paleoseismic and historical records indicate that the DSF has been continuously active and was the source of several destructive earthquakes that shook the entire region throughout geological times (Begin, 2005). Over the past two centuries, large earthquakes with intensities reaching X on the Modified Mercalli (MM) scale occurred in the area. The earthquake of October 30, 1759 (Amiran *at al.,* 1994) located probably in southern Lebanon, affected most of today's Lebanon, Israel and Syria with damage occuring as far south as Jaffa. Some sources report a death toll of 10,000 - 40,000 people. According to Ambraseys and Barazangi (1989) losses were certainly considerable. The earthquake that occurred on January 1, 1837 was the strongest earthquake in the region since the 19th century (Amiran *et al*., 1994), where most of the damage reported was in Safed and Tiberias. The July 11, 1927 earthquake, with magnitude M=6.2, was the most destructive regional seismic event in the 20th century. The effects of that earthquake were devastating, particularly in Jerusalem and in the towns of Lod and Ramle. In Lod and Ramle, which were small towns at that time, many buildings were destroyed and 50 people were killed (Avni *et al*., 2002). We note that these towns are relatively distant from the epicentre i.e., about 60 km. In the earthquake of January 749, with possibly a similar magnitude,

the flourishing Roman-Byzantine town of Bet Shean was destroyed. Fig. 1 presents mapped active faults (after Bartov *et al*., 2002) along with the suggested epicentres of historical earthquakes (after Ben-Menahem, 1979) and the earthquake epicentre of July 11, 1927 (Shapira *et al*., 1993).

Seismic wave amplification due to sedimentary deposits overlying hard rock is one of the more important parameters influencing seismic hazard. Site effects associated with ground motion amplification at resonance frequency of a building may have severe consequences. In the last decade, the Geophysical Institute of Israel has launched a number of projects to identify and map areas which are expected to amplify seismic ground motions across Israel (i.e., Zaslavsky *et al*., 1995, 2000; Shapira *et al*., 2001). In those studies, we used various empirical methods to study the site response, including reference (Borcherdt, 1970; Kagami *et al*., 1982) and non-reference (Lermo and Chávez-García, 1993) techniques as well as different sources of excitation: earthquakes, explosions and ambient noise (Zaslavsky *et al*., 2003).

Nakamura (1989, 2000) proposed a method to estimate the site effect by horizontal-to-vertical (H/V) spectral ratios of ambient noise. In a recent comprehensive study by SESAME European project (Atakan *et al*., 2004; Bard *et al*., 2004) of Nakamura's method it was concluded that the H/V spectral ratio of ambient noise corresponds to first resonance frequency of the site but the H/V amplitude is not necessarily the expected amplification of shear waves but may serve as a lower bound of the expected amplification levels. Studies of Zaslavsky *et al*. (2000, 2005, 2006) as well as many other investigators (Toshinawa *et al*., 1997; Chávez-García and Cuenca, 1998; Mucciarelli *et al*., 2003) showed that H/V spectral ratio obtained from ambient noise can be used to obtain reliable information related to linear seismic behavior of sedimentary layers.

Dimona and Bet Shean represent a typical example of towns located close to active faults, where one should expect intensified damage due to local site conditions. Inferring site response by modelling is rather limited due to the lack of site specific geotechnical information and data from boreholes. In an attempt to develop subsurface models we compared observations from seismic surveys that were carried out in the study areas with observed H/V spectral ratios obtained from ambient noise measurements. The models derived are extrapolated over the study area and enable us to understand the spatial distribution of the expected amplifications and their associated fundamental frequencies. Consequently, we constructed a zonation map and associated each of the zones to a characteristic soil column model.

2. Geological framework

The town of Dimona is situated in the north-eastern part of the Dimona-Yeroham syncline having a hard carbonate basement of Late Cretaceous age. The geological map in Fig. 2a shows the lithological units exposed in the investigated area (Roded, 1996). According to information from a well, located more than 3 km SE of the investigated area, as well as a study of Harash (1967), the sedimentary section unconformably overlying the carbonate basement is represented from the bottom to the top by Neogene coarse sandstone and conglomerate of about 70 m thick, 30 m sand-sandstone-conglomerate-silt-clay sequences and Holocene soil, loess, clay, loam and gravel and are a few meters thick.

The town of Bet Shean is located around the junction of the aligned Harod-Bet Shean valleys

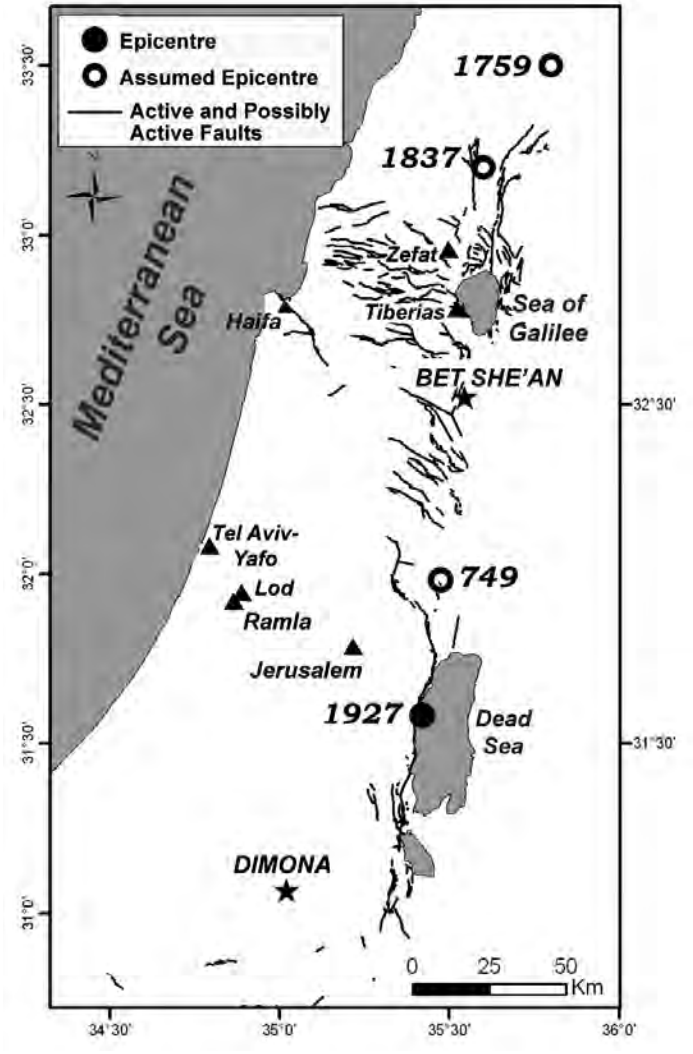

Fig. 1 - Location of assumed active faults and epicentres of historical earthquakes. The epicentre of the July 11, 1927 earthquake is marked by a full circle.

with the DSF (Fig. 2b). Two main fault systems were mapped in the Bet Shean area: NW-SE oriented lineaments that cross the Bet Shean valley and the western faults of the DSF. The stratigraphic section of the study area consists of Neogene fluvial-lacustrine sediments interbedded with volcanic and pyroclastic rocks. The Pliocene basalt flows of 50-150 m thick having a regional extension is assumed as bedrock. These rocks crop out in the northern part of the study area. Travertine of late Pleistocene age overlays the Pliocene basalt. The Bet Shean travertine is a rather local unit extending along a belt about 10 km long and 4-6 km wide in the N-S direction. According to Rozenbaum *et al*. (2004), the travertine is divided into two main facies: one is Phytoherm framestone and pyroclastic tufa facies further named "upper travertine" and the other is "intraclast tufa and Cyanolith "oncoidal" tufa (travertine). Holocene sediments mainly covering the western part of the study area are represented by colluvium, alluvium and anthropogenic sediments.

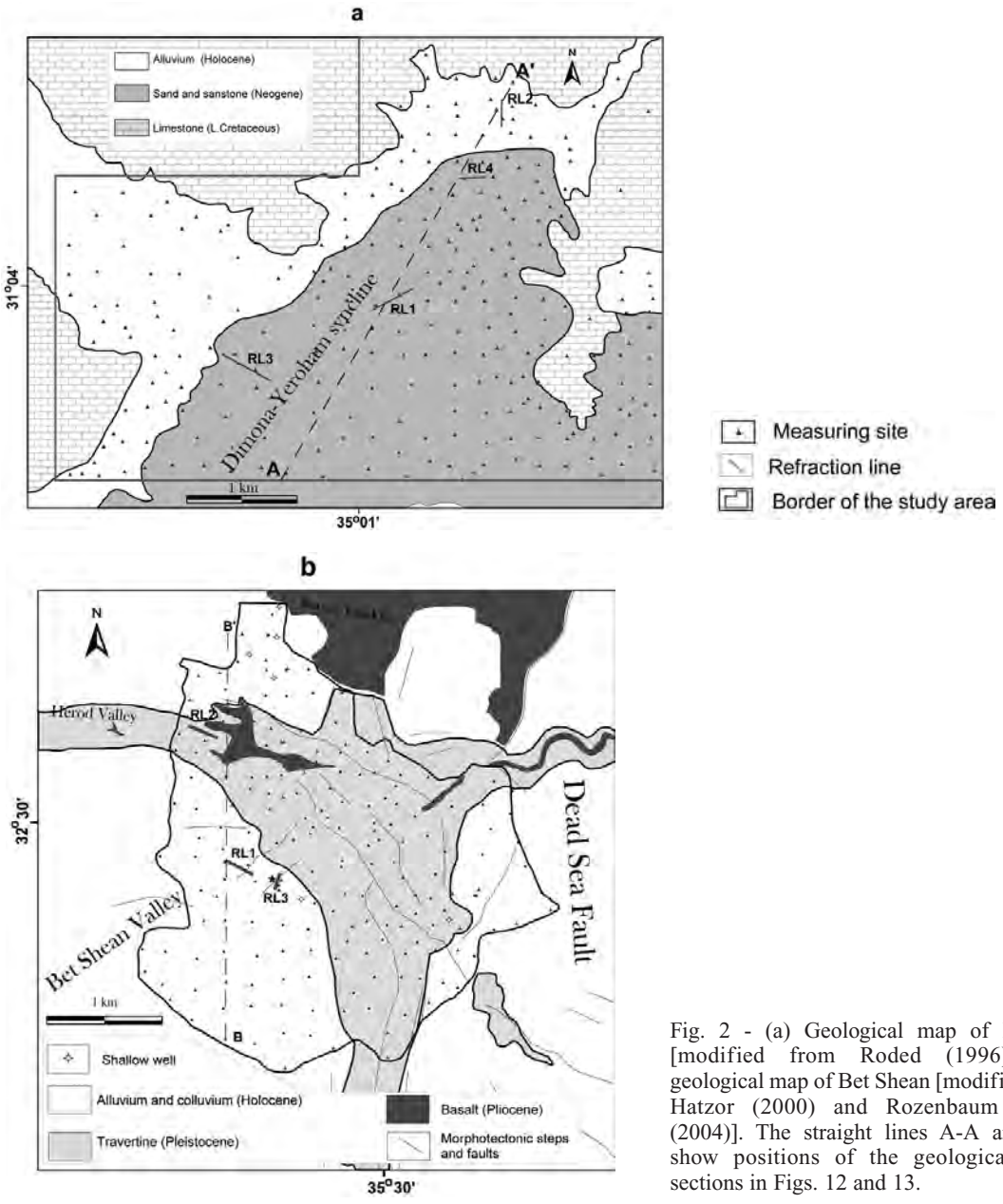

Fig. 2 - (a) Geological map of Dimona [modified from Roded (1996)]; (b) geological map of Bet Shean [modified from Hatzor (2000) and Rozenbaum *et al.* (2004)]. The straight lines A-A and B-B show positions of the geological cross sections in Figs. 12 and 13.

3. Observations and data processing

Ambient noise measurements were carried out during the period March to August 2004 in the town of Dimona and from May to September 2005 in the town of Bet Shean. The study areas are approximately 40 km^2 and 20 km^2 wide, respectively. The ambient noise was recorded at 275 sites in Dimona and 210 sites in Bet Shean (see Fig. 2). Ambient noise measurements are conducted using portable instruments (Shapira and Avirav, 1995) consisting of a multi-channel amplifier, a Global Positioning System (GPS) and a laptop computer with 16-bit analog-to-digital conversion card. Each seismograph station consists of

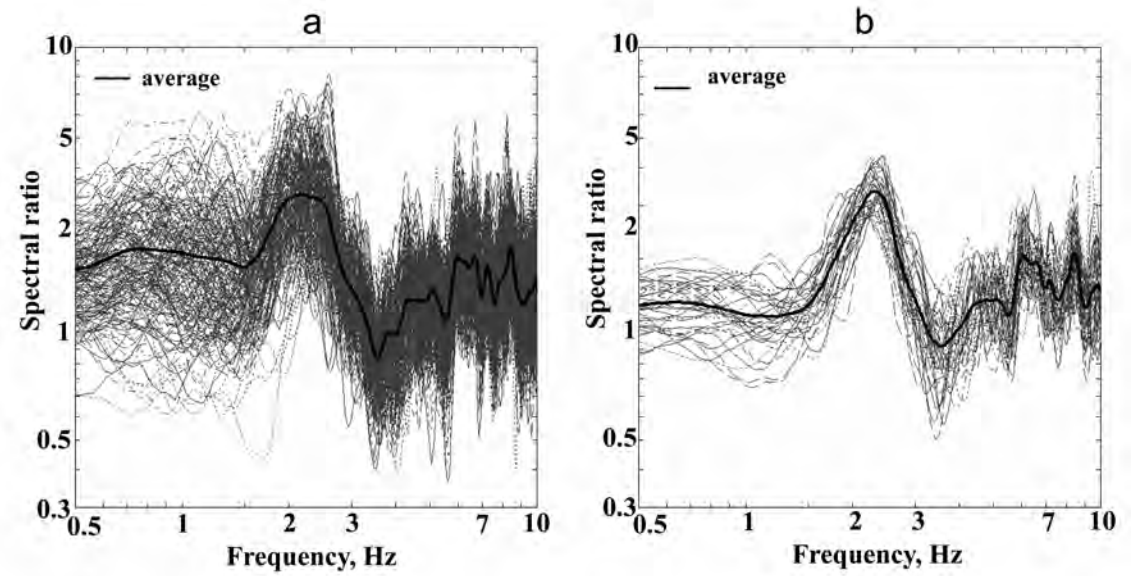

Fig. 3 - H/V spectra ratios of automatic (a) and manually (b) selected time windows.

three (one vertical and two horizontal) L4C velocity transducers (Mark Products) with a natural frequency of 1.0 Hz and damping ratio 70% of critical. The recorded signals are made at 100 samples per second and band-pass filtered between 0.2 Hz and 25 Hz.

Prior to performing measurements, the individual seismometer constant (natural-frequency, damping and motor constant) are determined using sine and step calibration signals, and then the frequency response function of all channels are computed. As a final test, all seismometers are placed at the same location, and in the same orientation, to record the same waves.

As already observed by many researchers, there is a high scatter in the H/V spectra. The source of the scatter is debated between the researchers. Mucciarelli (1998), for example, claims that traffic is not a major reason, whereas in their analysis, Horike *et al*. (2001) used recordings of microtremors originating from passing traffic. Recently, Parolai and Galiana-Merino (2006) showed that the influence of transients on the H/V spectral ratio is insignificant. Our observations also indicate that the effect of transients is almost unnoticeable. In order to reduce the scatter and increase stability, our processing scheme involved a careful selection of the time windows from which we obtained H/V functions. We adhered to the concept that at a site with no site effects the amplitude spectra of the H and V components of the ground motions are of the same level throughout the spectrum. At sites with significant site effects, the spectral amplitudes of the two components will differ only within a certain limited frequency band, probably in the neighbourhood of the resonance frequency. Time windows that exhibit such or similar conditions were selected. The selection was made manually, and yields an appreciated deduction in the H/V scatter. An example of spectral ratio estimates, obtained in Dimona from automatic and careful manual selection is shown in Fig. 3. Continuous records of ambient noise, for 60-70 minutes long enables us to select a sufficient number of suitable samples for analysis.

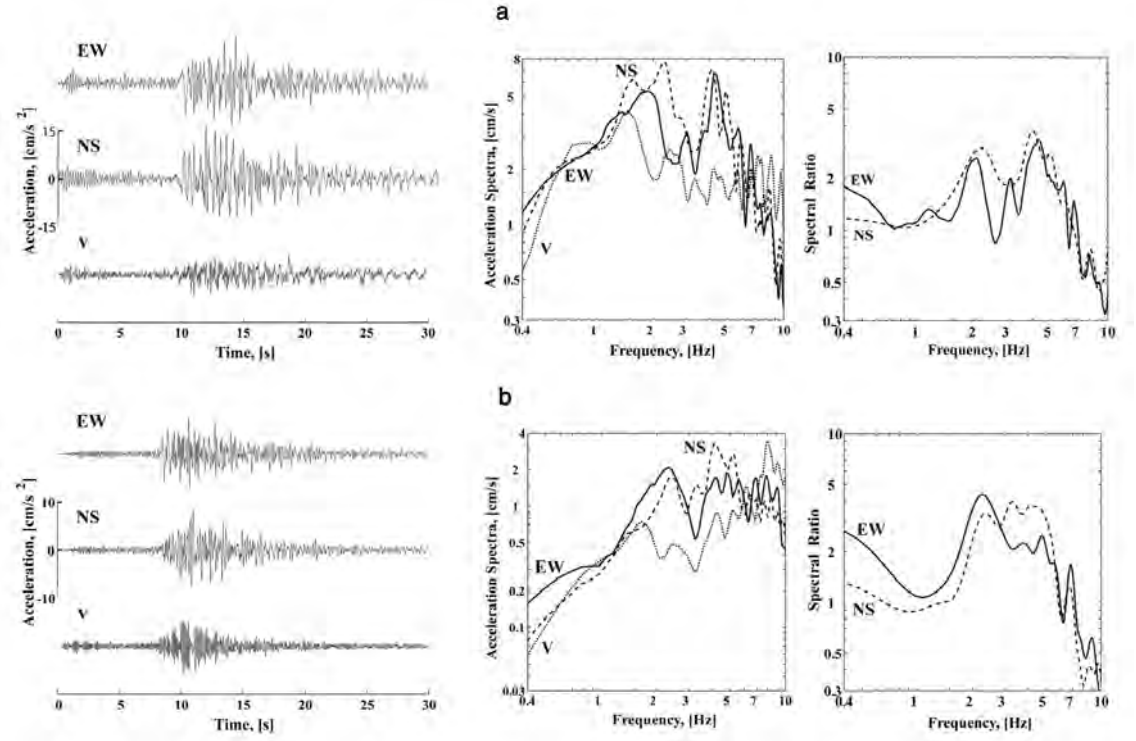

Fig. 4 - Accelerograms, their amplitude spectra and the spectral ratios recorded at the location of the Bet Shean strong motion station: (a) recordings of the earthquake of February 11, 2004; M_L=5.2, at epicentral distance of 90 km. (b) recordings of the earthquake of July 7, 2004; M_L=4.7, at an epicentral distance of 60 km.

For each site, we determined the average H/V spectral ratios and their corresponding standard deviations by applying the following process: time windows, each 30 seconds long, provided sets of H and V ground motions that were Fourier transformed using cosine-tapering (1 s at each end) before transformation. The spectra were then smoothed with a triangular moving Hanning window. More precisely, we applied a "window closing" procedure (see Jenkins and Watts, 1969) for smart smoothing of spectral estimates so that any significant spectral peaks are not distorted. For each site, we compiled a set of up to 50 selected time windows, each window providing an H/V spectral function.

The average spectral ratio for each of the two horizontal components is computed; if the curves of average spectral ratios of the two components are similar then the average of the two H/V ratios is defined as:

$$A(f)=\frac{1}{2n}\left[\sum_{i=1}^{n}\frac{S_{NS}(f)_i}{S_V(f)_i}+\sum_{i=1}^{n}\frac{S_{EW}(f)_i}{S_V(f)_i}\right] \quad (1)$$

Where $S_{NS}(f)_i$ and $S_{EW}(f)_i$ are individual spectra of the horizontal components and $S_V(f)_i$ is an individual spectrum of the vertical component.

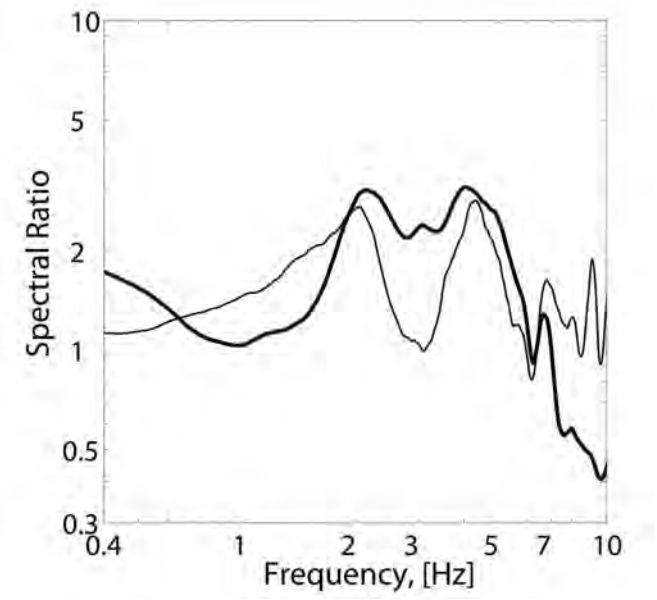

Fig. 5 – The average H/V spectral ratios observed at Bet Shean strong motion station: the thick line refers to the average composed of the H/V ratios from two earthquakes; the thin line is obtained from ambient noise measurements.

4. H/V spectral ratio

4.1. Comparison of H/V spectral ratios obtained from ambient noise and seismic events

The Seismology Division of the Geophysical Institute of Israel operates 62 strong motion stations. Two earthquakes on February 11, 2004 (M_L=5.2) and July 7, 2004 (M_L=4.7), that occurred in the DSF system, triggered 24 and 14 accelerometers, respectively, including one located in Bet Shean. In Fig. 4, we compare accelerograms of the two earthquakes, their spectra and spectral ratios. In the time domain there is a noticeable difference in the frequency content of the shear waves in the vertical components, the Fourier spectrum shows that the accelerogram of the July 7, 2004 earthquake is enriched with motions of higher frequencies with a peak near 8 Hz. The H/V ratios of two horizontal components of the accelerograms of the first earthquake (Fig. 4a) show two prominent peaks near 2 Hz and 4 Hz with amplitude ratio 3-3.5. The H/V ratios from the second earthquake (Fig. 4b) clearly exhibit the resonance peak near 2 Hz with an amplitude reaching 4 for the E-W component. At the N-S component, we can see amplification in the frequency range 2-5 Hz. with corresponding amplitude of about 3. Fig. 5 shows the average H/V spectral ratios for the N-S and E-W components obtained from two earthquakes and from the ambient noise both of which were recorded at the same site. There is a clear agreement in the location and amplitude of the two maxima between the functions obtained from the different data sets.

When conducting ambient noise measurements in Dimona, we recorded three explosions from quarries located 15 and 115 km from the measured site with corresponding magnitudes of 2.0 and 2.7, respectively. In Fig. 6, we compare the averaged H/V spectral ratios of the two horizontal components, obtained at 3 sites from seismograms of the explosions and from ambient noise. Note that site 87 is located on an outcrop of hard rock and as expected, the H/V functions imply no amplification effects at this site. Sites 9 and 129 are located on sediments. Also note that the

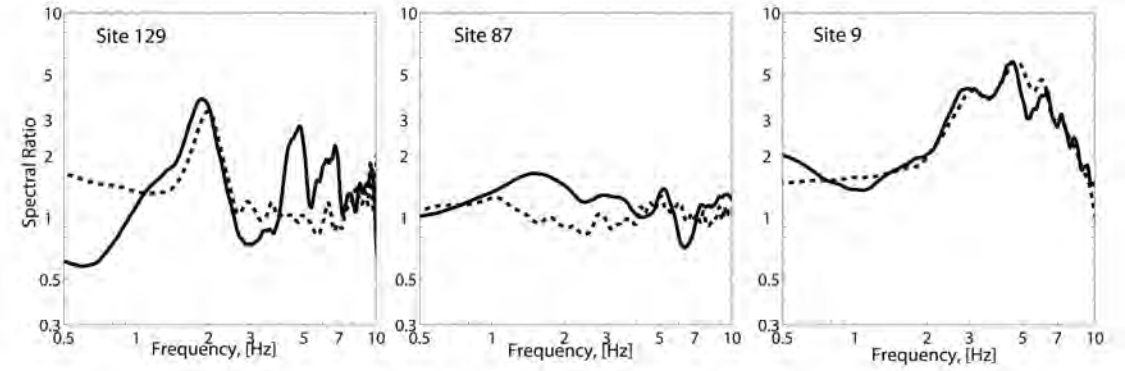

Fig. 6 - H/V spectral ratios at three sites in Dimona obtained from seismogram of explosions (solid line) and from ambient noise measurements (dashed line).

spectral ratios of the explosions and the noise measurements are very similar.

4.2. Fundamental resonance frequency and its spatial distribution

The fundamental frequencies or else the first resonance frequencies of the H/V functions obtained from the ambient noise measurements in Dimona and their associated H/V amplitudes are assembled to form the contour maps in Fig. 7. The fundamental frequencies in the town of Dimona are in the range of 1.5-9 Hz (see Fig. 7a). At sites located on outcropping limestone and dolomite of the Late Cretaceous age and also, at sites the adjoining belt, up to 600 m wide, we could not detect a prominent frequency that implies no amplification. The fundamental frequency decreases gradually from 5-10 Hz to 3 Hz towards the axis of the Dimona-Yeroham syncline striking SW-NE. This is in accordance with the geological map of the area (see Fig. 2). The asymmetrical shape of the syncline is distinctly visible in the contours of the resonant frequency. However, the contour maps show another linear structure, which is indicated by the belt of lower

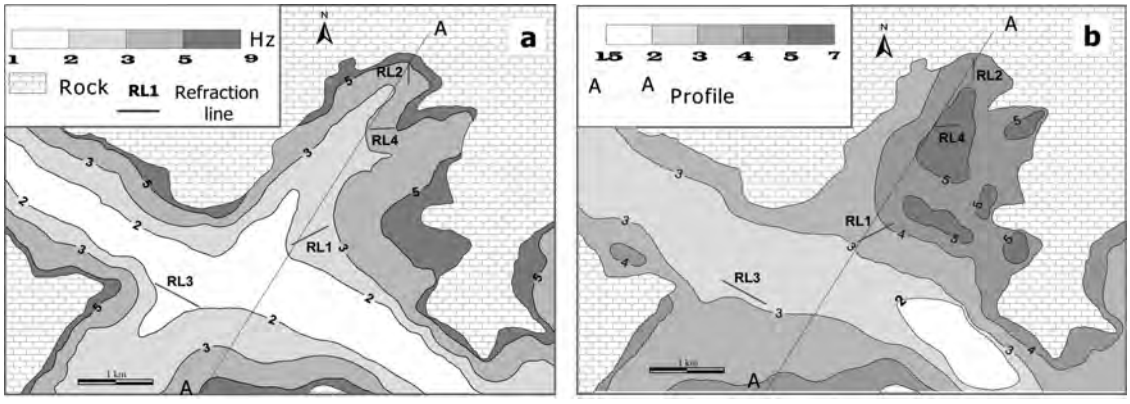

Fig. 7 - Distribution of the fundamental frequency (a) and its associated amplitude level (b) in Dimona.

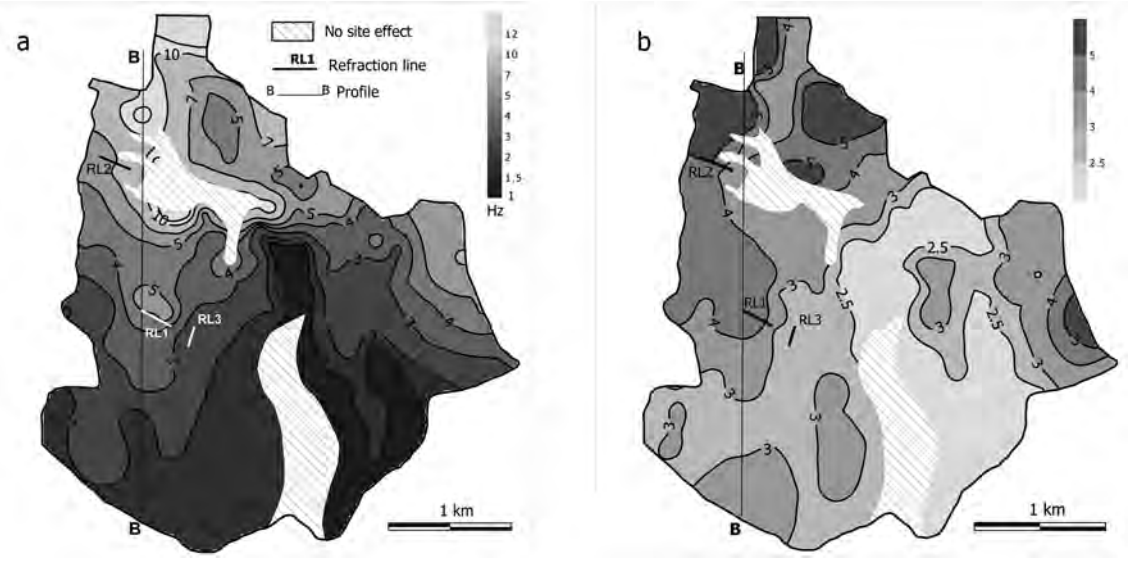

Fig. 8 - Distribution of the fundamental frequency (a) and its associated H/V amplitude (b) in Bet Shean.

fundamental frequency values (1-2 Hz) and is directed NW-SE. This structure confirms the paleogeographical reconstruction (Garfunkel and Horowitz, 1966) showing erosion channels connected by a river system of Miocene age.

Fig. 7b displays contours of the maximum H/V ratios varying from 2 to 10. The highest amplitudes (more than 5) are attained at sites located in the northeastern part of the study area. The smaller values (less than 3) are obtained in the already mentioned channel erosion of paleorelief filled by the carbonate-cemented conglomerate.

The prominent feature of the frequency and H/V amplitude maps in Bet Shean (Fig. 8) is a sub-meridional strike of isolines that coincide with main direction of the young active faults in the Bet Shean area. Fundamental frequencies vary within a wide range of 0.9-14 Hz. The higher frequencies are observed in areas surrounding the basalt outcrops at the northen edge of the town. General decrease in the resonance frequency toward the south and SE is correlated with the increasing depth to the basalt layer. We did not detect site amplification in two areas. One of these areas is associated with the exposed basalt and its adjacent sites made of a very thin layer of soft sediments overlying the hard rock. The other area that does not exhibit site effects, is adjacent to the western part of the DSF and may be associated with the absence of sharp changes in the seismic impedance in the ruptured zone along the faults. This is also supported by the seismic-reflection survey carried out in the southern outskirts of Bet Shean (Bruner *et al*., 2002).

The distribution of the maximum H/V amplitudes within Bet Shean is depicted in Fig. 8b. The highest amplification values (up to a factor 6) are at sites where soft alluvial deposits directly overlay the basalt, forming high seismic impedance. Moderate H/V levels (range from 2.5 to 4) are observed in areas where the lithological section consists of alluvium and travertine over the basalt. The sites showing low amplification (less than 2.5) are characterized by the travertine with high seismic wave velocity overlying the basalt.

Table 1 - Suggested one dimensional soil column model at sites near the seismic refraction lines in Dimona.

Refraction line	Lithology	Thickness (m)	V_s (m/s)	Density (g/cm^3)	Damping (%)
RL-2	Alluvium	20	440	1.7	3
	Conglomerate	10	1100	2.1	1
	Limestone, dolomite	-	2000	2.4	
RL-4	Alluvium	10	280	1.6	4
	Sandstone	40	600	1.8	2
	Limestone, dolomite	-	2000	2.4	
RL-1	Alluvium	20	400	1.7	3
	Sandstone	35	700	1.8	2
	Conglomerate	25	1100	2.1	2
	Limestone, dolomite	-	2000	2.4	
RL-3	Alluvium	10	350	1.7	4
	Sandstone	40	700	1.9	2
	Conglomerate	100	1100	2.0	1
	Limestone, dolomite	-	2000	2.4	

5. Supporting information from seismic refraction surveys

Data collected from a few seismic refraction lines, which were carried out in the investigated area, provide information about the S-wave velocities in the bedrock and in the upper sediments. Refraction lines (for location see maps in Fig. 2) are designed to obtain maximum information about V_s of the lithological units present in the study area.

Thickness of the layers in the town of Dimona and their V_s are given in Table 1. Densities and specific attenuation in different lithological units were chosen on the base of different sources of literature (Borcherdt *et al*., 1989; McGarr *et al*., 1991; Theodulidis *et al*., 1996; Pergalani *et al*., 2000; and many others). Recently, Pratt and Brocher (2006) used spectral decay in the shear-wave spectral ratio with respect to reference site amplification curves and estimated Q-values for shallow sedimentary deposits. They concluded that the range of Q values is 10-40. These values agree well with those, which are used in this study.

Interpretations of line RL-2 suggest a composition of three layers (Ezersky, 2006). Based on the data from a well, located 2 km from the study area and the geological-geotechnical reasoning, those layers are correlated with Holocene alluvium, Neogene conglomerate and limestone-dolomite of Cretaceous age. The analytical transfer function for that inferred soil sequence is in good agreement with the H/V spectral ratios obtained from ambient noise measurements at sites near line RL-2 and leading to the model presented in Table 1. RL-2 line is the only one of the available refraction lines reaching the fundamental reflector. Therefore, by analyzing the other refraction lines and using them for calculation of the transfer functions at corresponding locations, we take limestone-dolomite into account (V_s=2000 m/s) as the reflector. A layer

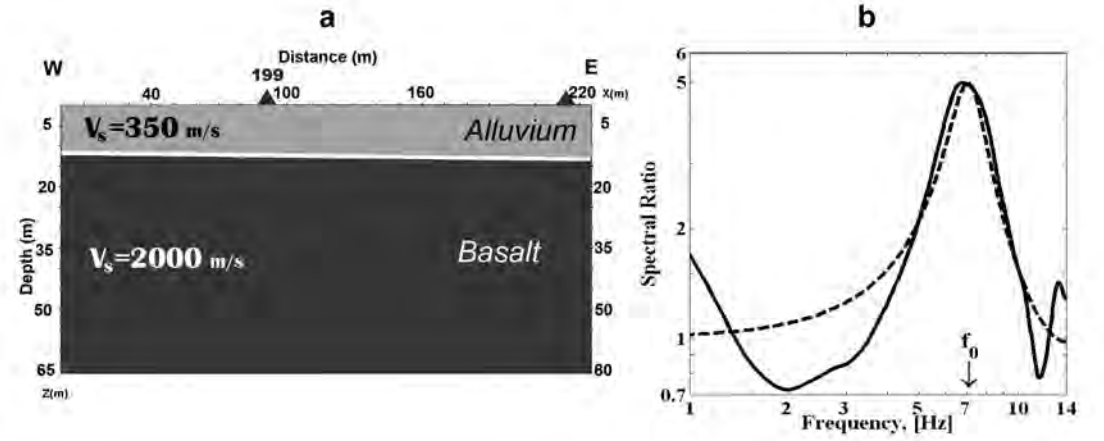

Fig. 9 - (a) Vertical cross section along line RL-2; (b) analytical transfer function (dashed line) compared with H/V spectral ratio (solid line) obtained at a site near RL-2

characterized by V_s=600-700 m/s appearing in three other refraction lines is correlated with Neogene sandstone.

Refraction line RL-2, in the town of Bet Shean, is located in the vicinity of the basaltic outcrop (see Fig. 2b). A vertical cross-section along line RL-2, presented in Fig. 9a, shows an upper layer 10-15 m thick (V_s=350 m/s) that overlies the basalt (V_s=2000 m/s). The analytical transfer function and the corresponding H/V spectral ratio of site 199 show a single peak at the fundamental frequency f_0 = 7 Hz (Fig. 9b).

Seismic refraction line RL-1 shows three layers which can be correlated to alluvium with V_s=280 m/s; travertine with V_s=1100 m/s and the basalt with V_s=2000 m/s (see Fig. 10a). The

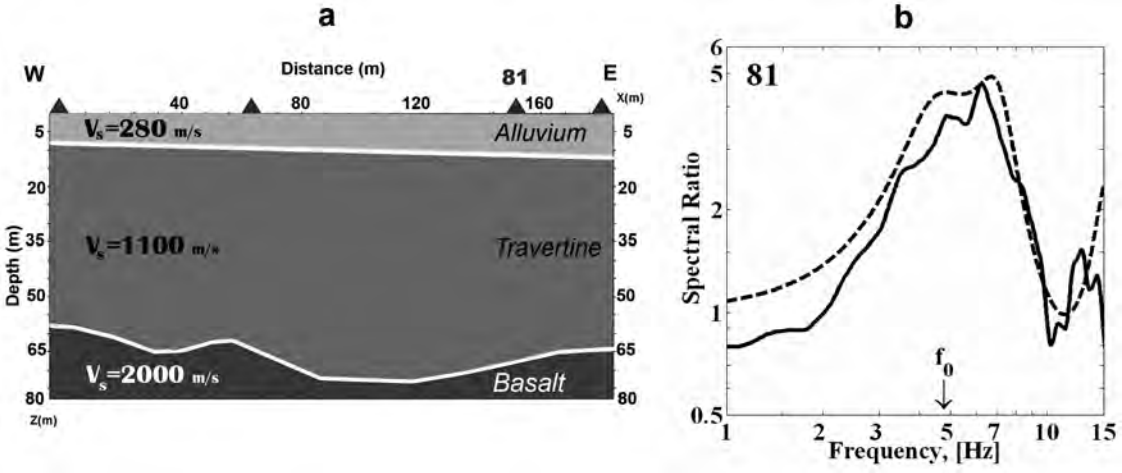

Fig. 10 - (a) Vertical cross section along line RL-1; (b) analytical transfer function (dashed line) compared with H/V spectral ratio (solid line) obtained at site 81. Triangles indicate measurement sites near RL-1.

Table 2 - Subsurface models along line RL-3 inferred from seismic refraction survey, down-hole velocity measurements and the suggested 1D soil column in Bet Shean.

Layer	Refraction data		Down-hole measurements		Suggested 1D model of the soil column	
	Thickness (m)	V_s (m/s)	Thickness (m)	V_s (m/s)	Thickness (m)	V_s (m/s)
1	4	300	6		5	300
2	12	550	6	625	30	600
			6	660		
3	15		6	570		
			6	640		
4	-	1000	-		60	1000
5					Half-space	2000

averaged H/V spectral function obtained for site 81 near the RL-1 line is shown in Fig. 10b. It exhibits a fundamental peak, at 4.5 Hz. The prominent feature of this curve, typical also for the other sites along this line, is a wide band of resonance frequencies which is in fair agreement with the 1-D theoretical transfer function computed using the information from the refraction line (Fig. 10b).

The RL-3 seismic refraction line is situated close to the location of the accelerometer. A series of down-hole measurements in the nearby shallow BH-1 well (Ezersky and Shtivelman, 1999) were performed. Well BH-1 is drilled to a depth of 30 m, passes through the alluvium and two travertine layers but does not reach the basalt. Down-hole velocity measurements are shown, together with the refraction data, in Fig. 11a and Table 2. Detailed estimations of the upper travertine velocity are averaged and used to construct a 1D soil column model. We note that the velocity of the travertine, V_s=1000 m/s, practically coincides with refraction measurements along line RL-1. Thickness of the travertine was taken from the geological source (Rozenbaum *et al*., 2004). The analytical transfer function that is based on the suggested 1D model and the observed H/V spectrum showing two separate peaks f_0 and f_1 associated with the fundamental (the basalt) and shallower (the travertine) reflectors, are presented in Fig. 11b.

Table 3 summarizes the characteristic S-wave velocities of the lithological units in the Bet Shean area.

6. Construction of subsurface 1D model

Many authors assume ambient noise is primarily composed of surface waves (Lachet and Bard, 1994; Konno and Ohmatchi, 1998; Arai and Tokimatsu, 2004). Consequently, the comparison of H/V ratio from ambient noise with the transfer function of S-waves is problematic. Others such as Nakamura (2000), Zhao *et al*. (2000), Enomoto *et al*. (2000) and Mucciarelli and Gallipoli (2004) claim that the H/V spectrum of ambient noise is dominated by the upward

Table 3 - Ranges of S-wave velocities for lithological units present in the study area in Bet Shean.

Lithology	V_s (m/s)
Alluvium	250-350
Upper Travertine	600-750
Travertine	1000-1200
Basalt	2000

propagation of the SH wave through the layered media. Whoever is right, both models agree that the H/V spectra and the site response function for the SH wave are the results of the velocity structure of the media, that both exhibit the same fundamental resonance frequencies with similar amplitudes at least when considering small motions. The authors of this study demonstrated, through many previous studies where noise measurements were made near boreholes and/or near refraction surveys, that the fundamental frequency and its corresponding H/V amplitude derived from the analysis of ambient noise are practically the same as the fundamental frequency and its corresponding amplification level derived from the computed transfer function of SH waves at low strains propagating through a relatively simple 1-D model of the site, known from geo-technical and geophysical surveying. Therefore, in order to construct models of the subsurface, we may start at sites close to refraction lines and boreholes, where we have subsurface information. Then propagate by means of extrapolation to neighbouring sites, using H/V spectral observations and information about the regional geology to constrain S-wave velocities of the lithological units present in the study area.

The stochastic optimization algorithm (Storn and Price, 1995) is applied in order to fit an analytical transfer function to an observed H/V spectrum, giving the same weight to the fundamental and second natural frequencies and by considering their amplitudes.

Fig. 12 depicts H/V spectral ratios for representative sites located along profile A-A in the town of Dimona, together with the corresponding analytical response functions that were computed for the suggested 1D model beneath each site. These compose a simplified sketch of the geological cross-section in a SW-NE direction i.e., a cross-section that is constructed by integrating results from the analysis of ambient vibration measurements. Analytical site response

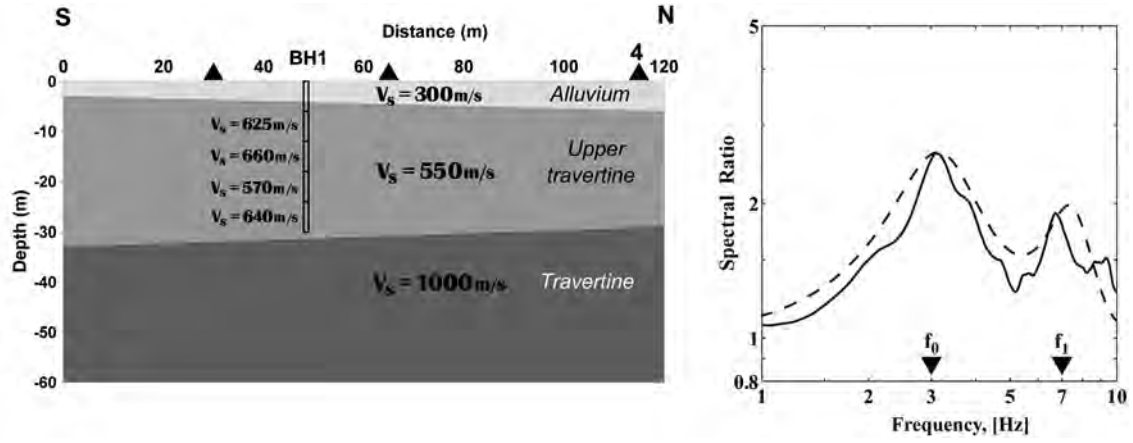

Fig. 11 – (a) Vertical cross section along line RL-3; (b) the analytical transfer function that is based on the suggested 1D model (dashed line) at line RL-3 and the observed H/V spectrum (solid line).

Table 4 - Thicknesses of layers derived using H/V ratios along profile A-A' in Dimona.

Lithology	**Measuring site**											
alluvium	245	226	97	104	161	162	81	122	94	269	5	163
	Thickness inferred from optimization procedure (m)											
alluvium	10	10	10	10	15	20	15	15	10	10	12	20
sandstone	15	40	45	55	50	40	30	45	40	40	30	--
conglomerate	15	30	85	110	60	25	25	--	--	--	25	35
limestone-dolomite	Depth to bedrock (m)											
	40	80	140	175	125	85	70	60	50	50	67	55

functions as well as observed H/V spectra for sites located along profile A-A show fundamental frequencies ranging from 1.5 to 5.5 Hz. According to the analytical functions, these are associated with amplification factors of 2-5. The prominent feature characterizing the A-A profile, is a decrease in both the fundamental frequencies and the amplitudes from the edges to the centre which is associated with an increase of the thickness of the sediments. Location of the profile along the syncline axes implies that the thicknesses of the alluvium and sandstone layers, obtained directly from the refraction data, does not change significantly along the profile. Consequently, the main variation in thickness above the reflector is attributed to the thickening of the conglomerate layer (V_s=1100 m/s) between points 98 and 162 in the erosion paleo-channel, crossing the Dimona-Yeroham syncline. Model parameters for a number of measurement sites are given in Table 4.

Reconstruction of the subsurface structure in Bet Shean is illustrated by the geological cross-

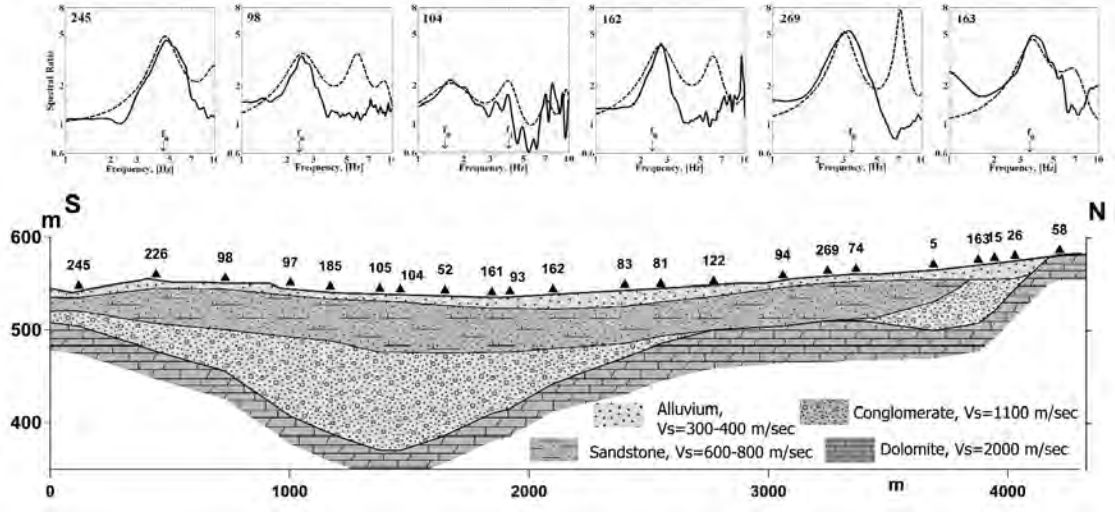

Fig. 12 - H/V spectral ratios (the solid line) and analytical transfer functions (the dashed line) for representative sites along profile A-A in Dimona and simplified sketch of the geological cross-section.

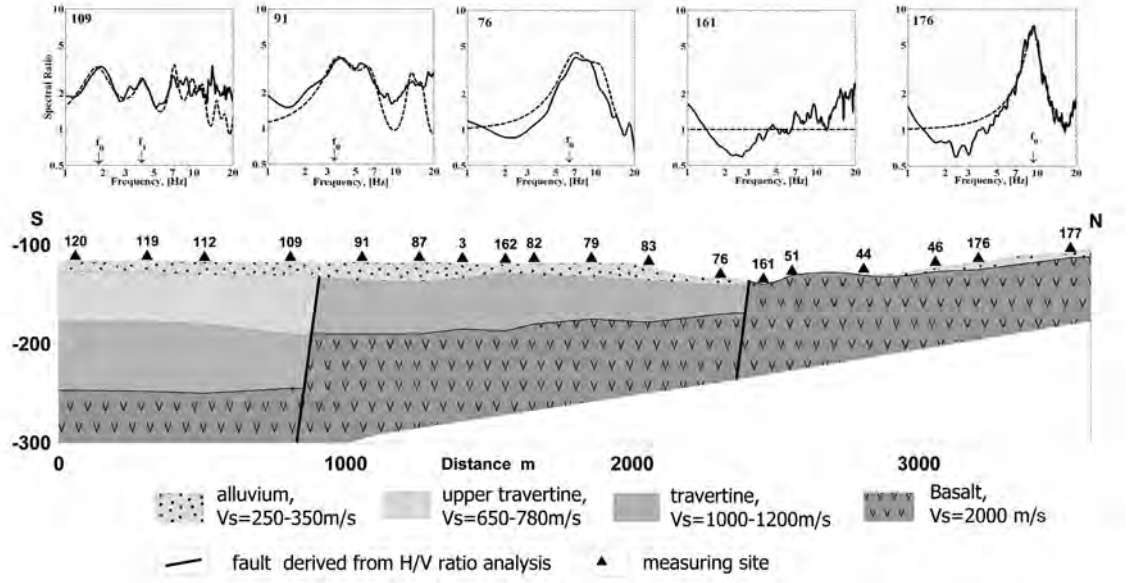

Fig. 13 - H/V spectral ratios (the solid line) and analytical transfer functions (the dashed line) for sites along profile B-B and a schematic geological cross-section in Bet Shean.

section B-B directed S-N (Fig. 2b). Fig. 13 shows H/V spectra for representative sites along the profile and the schematic geological cross-section. The H/V spectrum for site 109 represents the southern part of the profile. It exhibits a fundamental peak at 1.7 Hz and a minor one at 4 Hz. The analytical transfer functions for this, and surrounding sites, are calculated based on a velocity model derived from the seismic refraction line RL-3 located nearby (see Fig. 11). Site 91 exhibits a flat H/V spectral shape over a relatively wide frequency range. This is a result of two close resonance frequencies. The vertical cross-section shows that sites 109 and 91 are located at the two sides of a fault which is detected by a sharp change in the fundamental frequency from 1.7 Hz at site 91 to 3.5 Hz at site 109 corresponding to a vertical displacement (thickening of the sediments) of about 100 m. Moreover, changes in the shape of the H/V curve and amplitude level of the peaks indicate that there is a change in the velocity model. Based on the refraction survey, we should note that in the central part of the profile the upper travertine layer is absent. From site 91 to site 76 there is a gradual increase from 3.5 Hz to 7 Hz, which corresponds to the decrease of the total sediment thickness from 70 m to 40 m. Since the H/V spectral amplitudes do not change, in keeping a ratio of 4, we can conclude that there is no change in S-wave velocities.

The part of the profile north of site 161 runs through a basaltic outcrop. This is manifested in the H/V spectrum of site 161 that is almost flat in the whole frequency range. Also note that the abrupt change in the H/V spectra of 76 and 161 is due to the fault that runs between these sites. At the northern end of the profile (e.g. site 176) we observe high H/V amplitudes (almost a ratio of 10) at a high frequency (8-14 Hz) which is due to the few meters of alluvium overlying the basalt.

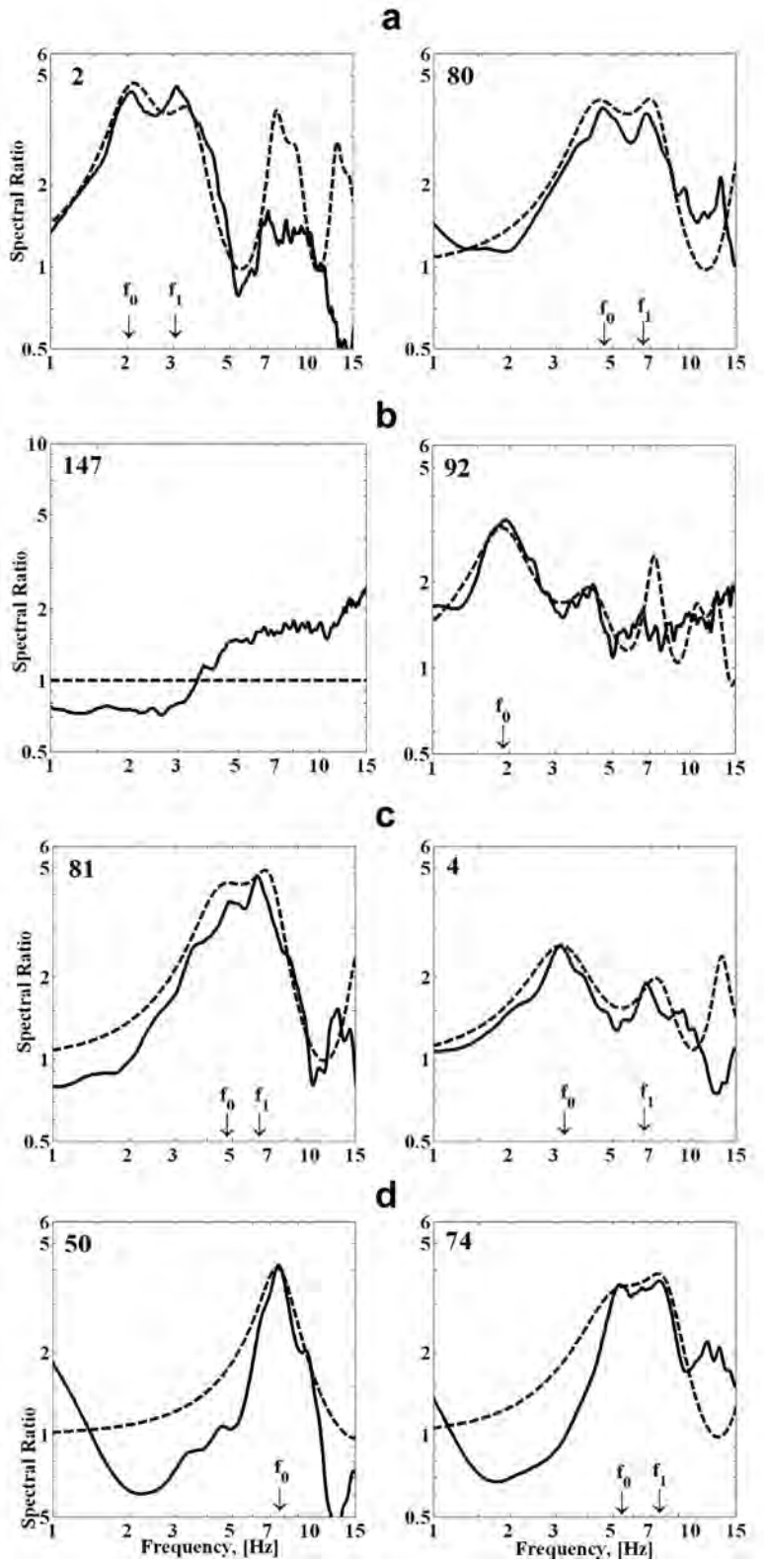

Fig. 14 - H/V spectral ratios (the solid line) and analytical transfer functions (the dashed line) for adjacent sites located at the different sides of fault: (a) the similar general shape of the H/V ratios but with a sharp shift in the fundamental frequency corresponds to a vertical displacement of about 60 m; (b) H/V ratio at the hard-rock site vs. the neighbouring resonating one; (c) and (d) significant difference in all three characteristics of the H/V spectra, i.e. fundamental frequency, amplitude and shape is associated with both a vertical displacement and change in the velocity profile.

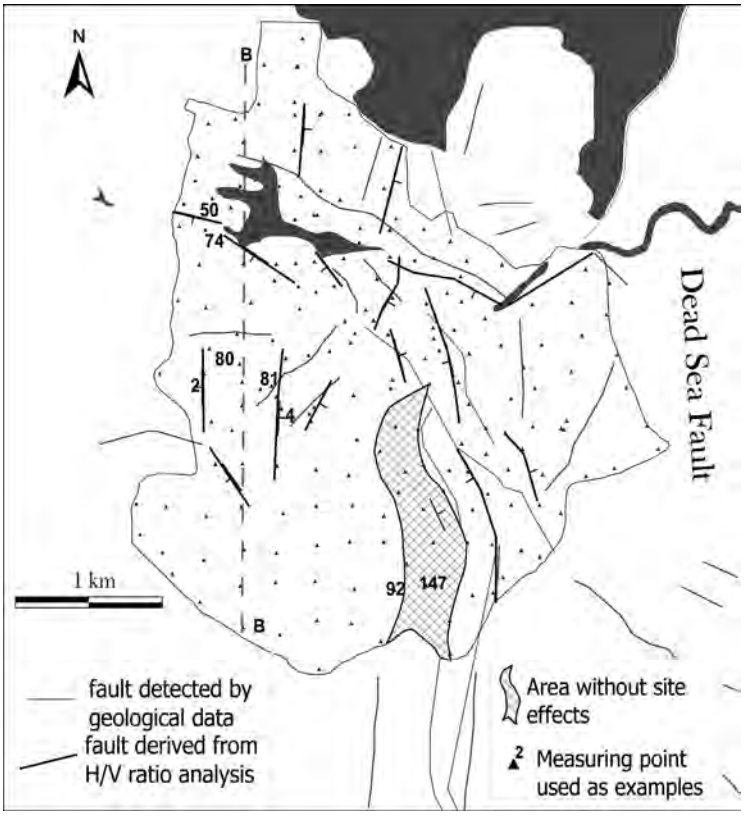

Fig. 15 - Map showing faults inferred from H/V analysis and faults mapped by using surface geology information.

7. Identification of faults

As already noted, a discontinuity in the subsurface is associated with either a sharp change in the fundamental frequency and/or a change in the shape of the H/V ratio over a short distance. This is likely to indicate the existence of a fault. Such situations have been identified at several places in the Bet Shean area. Examples are presented in Fig. 14.

Fig. 14a illustrates a case where the general shape of the H/V spectra at adjacent sites 2 and 80 are very similar but with a sharp shift of more than 2 Hz, i.e., the fundamental frequency at site 2 is 2.2 Hz and at site 80 it is 4.5 Hz. The two are located on both sides of a fault. The derived subsurface models suggest a vertical displacement of about 60 m. In Fig. 14b, we have an example where site 147 shows no resonance while the neighbouring site 92 resonates with a fundamental frequency of about 2 Hz. A similar example is presented in Fig. 13 and is associated with a mapped fault. The examples in Fig. 14c and Fig.14d represent cases, rather common in the study area, when all three characteristics of the H/V spectral function, i.e. fundamental frequency, amplitude and shape are different. Such occurrences are probably associated with vertical displacement and a change in the velocities (possibly different material). The observed changes between sites 81 and 4 (Fig. 14c) are explained by a fault running between these sites. The fault is associated with a vertical displacement of about 50 m. One side of the fault has alluvium-

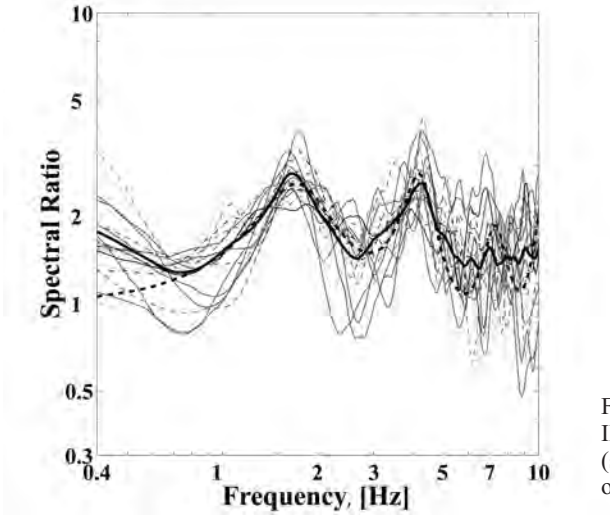

Fig. 16 - H/V spectral ratios from different sites in Zone II in Bet Shean (thin lines), the average H/V spectrum (solid line) and analytical transfer function for Zone II of Bet Shean (dashed line).

travertine overlying the basalt while the other side has alluvium - upper travertine - travertine overlying the basalt. A similar transition from alluvium - basalt structure to alluvium - travertine - basalt occurs between sites 50 and 74 (Fig. 14d).

The map in Fig. 15 presents faults inferred from the analysis of ambient noise measurements and faults already mapped by other geological means. The NW-SE and N-S oriented lineaments are distinguished in the study area. The estimated vertical displacement judged from the depth to the hard rock surface (the main seismic wave reflector) is 30-50 m in the centre up to 100 meters in the south of the study area. Faults having a N-S strike are associated with younger tectonic activity of late Pleistocene age and generally coincide with the western faults of the DSF.

8. Microzonation

Subsurface models were developed by means of integrating information from empirical H/V spectra, available geological data and geophysical refraction data. These models in turn, are used for seismic hazard microzonation across the study area. The grouping is done manually taking into consideration the fundamental frequency, H/V amplitude and the shape of the response functions. An example, showing the assembly of H/V spectra, the averaged H/V spectrum and the analytical response function for Zone II in Bet Shean is shown in Fig. 16.

Seismic microzoning maps, presenting zones of common site effect characteristics were prepared for the towns of Dimona (Fig. 17) and Bet Sean (Fig. 18). Figs. 17 and 18 also describe the generalized 1D soil columns that are associated with each zone, which in turn, can be used for assessment of the expected ground shaking.

9. Discussion and conclusions

Damage caused to a structure can be extensive if the ground shaking contains frequencies that

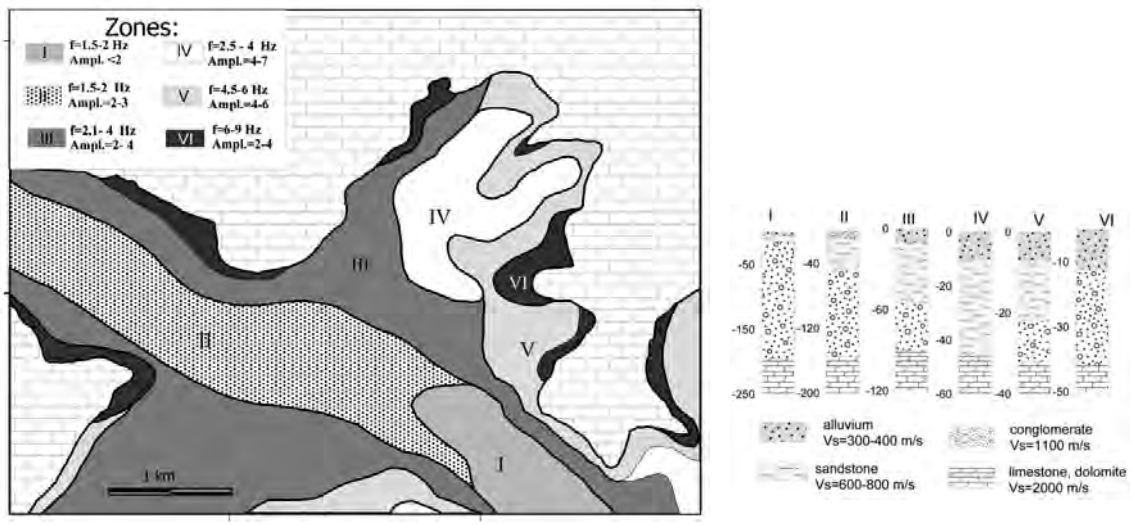

Fig. 17 - Seismic microzoning map of Dimona, presenting zones of common site effect characteristics and the 1D soil column models for each zone.

are at the natural frequencies of the structure. The types of buildings currently characterizing the residential building stock in Dimona and Bet Shean are prefabricated structures with 3-4 stories having a rectangular floor plane and different width-to-length ratio, designed in the late 1970's.

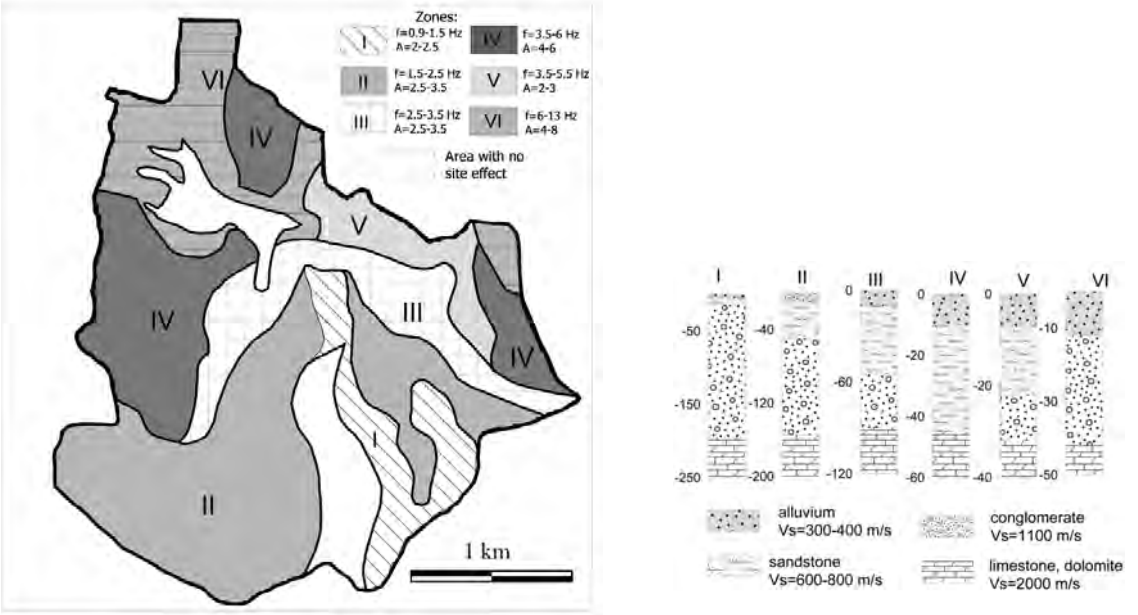

Fig. 18 - Seismic microzoning map of Bet Sean, presenting zones of common site effect characteristics and the 1D soil column models for each zone.

We conduct a series of seismological measurements in the low-rise buildings in Dimona and observed the natural frequencies of the buildings to be in the range of 3.5 to 6.0 Hz. We should emphasize that the densely populated quarters in both towns are located in zones where seismic ground motion in the frequency range of 3-6 Hz are expected to be significantly amplified during earthquakes. Further investigation should be carried out in order to better assess the vulnerability of existing building and the associated earthquake risk.

This study demonstrates the significantly added value of performing ambient noise measurements over a dense grid of measuring sites and improve possibilities to calibrate and correlate seismological information with information from different sources; e.g. surface geology, seismic refraction and reflection surveys, borehole data, geotechnical information and more. Such an integrated study is likely to produce a coherent and systematic assessment of the seismic hazard prevailing in the study area.

To avoid any misunderstanding, we should emphasize that the analytical transfer functions discussed in this study are only associated with weak motions, in the range where the behaviour of the soils is linear. Therefore, these functions do not represent the site effects under strong ground motion. The nonlinear characteristics of different sites within Dimona and Bet Shean are beyond the scope of this study. Nevertheless, based on the result presented above nonlinear site response can be determined by different mathematical models of soil nonlinearity, making use of the models developed for each zone. In that respect, the microzonation maps developed in this study are also relevant for the prediction of ground motions from earthquakes of high magnitudes.

Acknowledgments. Our thanks go to the Ministry for Absorption and to the Earth Sciences Research Administration of the Ministry for National Infrastructure for their financial support. The studies were conducted under Contracts No. 23-17-023 and No. 24-07-017. The authors are grateful to V. Avirav for helping with the data processing. Preliminary results of this study were presented at the First European Conference on Earthquake Engineering and Seismology, September 3-8, 2006, Geneva, Switzerland.

REFERENCES

Ambraseys N.N. and Barazangi B.; 1989: *The 1759 earthquake in the Bekaa Valley: implications for earthquake hazard assessment in the eastern Mediterranean region.* J. Geophys. Res., **94**, 4007-4013.

Amiran D.H.K., Arieh E. and Turcotte T.; 1994: *Earthquakes in Israel and adjacent areas: macroseismic observations since 100 B.C.*E. Israel Exploration Journal, **2**, 261-305.

Arai H. and Tokimatsu K.; 2004: *S-wave profiling by inversion of microtremor H/V spectrum.* Bull. Seism. Soc. Am., **94**, 53-63.

Atakan K., Duval A-M., Theodulidis N., Guillier B., Chatelan J-L., Bard P-Y. and the SESAME-Team; 2004: *The H/V spectral ratio technique: experimental conditions, data processing and empirical reliability assessment.* In: Proc. of 13th World Conf. of Earth Eng., Vancouver, Aug., 2004, CD-Rom.

Avni R., Bowman D., Shapira A. and Nur A.; 2002: *Erroneous interpretation of historical documents related to the epicentre of the 1927 Jericho earthquake in the Holy Land*. J. of Seismology, **6**, 469-476.

Bard P.-Y. and 76 SESAME participants; 2004: *The SESAME project: An overview and main results*. In: Proc. of 13th World Conf. of Earth. Eng., Vancouver, Aug., 2004, CD-Rom.

Bartov Y., Sneh L., Fleisher L., Arad V. and Rosensaft M.; 2002: *Map of fault in Israel.* Scientific Report GSI/29/2002, Geological Survey of Israel, 8 pp.

Begin Z. B.; 2005: *Destructive earthquakes in the Jordan Valley and the Dead Sea – their recurrence intervals and the probability of their occurrence.* Scientific Report GSI 12/05, The Geological Survey of Israel (Hebrew with summary in English), 32 pp.

Ben-Menahem A.; 1979: *Earthquake catalog for the Middle-East (92 B.C. – 1980 A.D.).* Boll. Geof. Teor. Appl., **21**, 245-310.

Borcherdt R. D.; 1970: *Effects of local geology on ground motion near San Francisco bay*. Bull. Seism. Soc. Am., **60**, 29-61.

Borcherdt R., Glassmoyer G., Andrews M. and Cranswick E.; 1989: *Effect of site conditions on ground motion and damage.* Earthquake spectra, Special supplement, Armenia earthquake reconnaissance report, 23-42.

Bruner I., Zilberman E. and Amit R.; 2002: *High resolution seismic refraction survey along the Bet Shean Fault.* Scientific Report GSI/37/2002, Geological Survey of Israel, 12 pp.

Chávez-García F. J. and Cuenca J.; 1998: *Site effects and microzonation in Acapulco.* Earthquake Spectra, **14**, 75-93.

Enomoto T., Kuriyama T., Abeki N., Iwatate T., Navarro M. and Nagumo M.; 2000: *Study on microtremor characteristics based on simultaneous measurements between basement and surface using borehole.* In: Proc. of 12th World Conf. of Eart. Eng., Auckland, January, 2000, CD-Rom.

Ezersky M., 2006: *Seismic refraction survey at the Dimona, Arad and Petah-Tikva areas for site response assessment.* Report No. 266/120/06, Geophysical Institute of Israel, 30 pp.

Ezersky M. and Shtivelman V.; 1999: *Seismic refraction surveys for updating the microzonation map of Israel.* Report No. 802/43/99, Geophysical Institute of Israel, 25 pp.

Harash A.; 1967: *The geology of Yeroham-Dimona Plain.* M. Sc. thesis, Hebrew University, Jerusalem, 72 pp.

Hatzor Y.; 2000: *The geological map of Bet Shean,* 1: 50 000, sheet 1. Geol. Survey of Israel.

Horike M., Zhao B. and Kawase H.; 2001: *Comparison of site response characteristics inferred from microtremors and earthquake shear wave.* Bull. Seism. Soc. Am., **91**, 1526-1536.

Garfunkel Z. and Horowitz A.; 1966: *The Upper Tertiary and Quaternary morphology of the Negev*. Israel J. Earth Scienc., **15**, 101-117.

Jenkins M. G. and Watts D. G.; 1969: *Spectral analysis and its applications.* Holden-Day, San Francisco, 1969, 471 pp

Kagami H., Duke C.M., Liang G.C. and Ohta Y., 1982: *Observation of 1- to 5-second microtremors and their application to earthquake engineering. Part II. Evaluation of site effect upon seismic wave amplification deep soil deposits.* Bull. Seism. Soc. Am., **72**, 987-998.

Konno K. and Ohmachi T.; 1998: *Ground-motion characteristics estimated from spectral ratio between horizontal and vertical components of microtremors*. Bull. Seism. Soc. Am., **88**, 228-241.

Lachet C. and Bard P.Y.; 1994: *Numerical and theoretical investigations on the possibilities and limitations of the Nakamura's technique.* J. Phys. Earth, **42**, 377-397.

Lermo J. and Chávez-García F. J.; 1993: *Site effect evaluation using spectral rations with only one station.* Bull. Seism. Soc. Am., **83**, 1574-1594.

McGarr A., Celebi M., Sembera E., Noce T. and Mueller C.; 1991: *Ground motion at the San Francisco international airport from the Loma Prieta earthquake, sequence.* Bull. Seism. Soc. Am., **81**, 1923-1944.

Mucciarelli M.; 1998: *Reliability and applicability of Nakamura's technique using microtremors: an experimental approach.* J. of Earth. Eng, **4**, 625-638.

Mucciarelli M. and Gallipoli M. R.; 2004: *The HVSR technique from microtremor to strong motion: empirical and statistical considerations.* In: Proc: of 13th World Conference of Earthquake Engineering, Vancouver, Aug., 2004, CD-Rom.

Mucciarelli M., Gallipoli M. R. and Arcieri M.; 2003: *The stability of the horizontal-to-vertical spectral ratio of triggered noise and earthquake recording.* Bull. Seism. Soc. Am., **93**, 1407-1412.

Nakamura Y.; 1989: *A method for dynamic characteristics estimation of subsurface using microtremor on the ground surface.* Quarterly Report of Railway Technical Research. **30**, 25-33.

Nakamura Y.; 2000: *Clear identification of fundamental idea of Nakamura's technique and its applications.* In: Proc. of 12th World Conf. of Eart. Eng., Auckland, January, 2000, CD-Rom.

Parolai S. and Galiano-Merino J.J.; 2006: *Effect of transient seismic noise on estimates on H/V spectral ratios.* Bull.

Seism. Soc. Am., **96**, 228-236.

Pergalani F., Romeo R., Luzi L., Petrini V., Pugliese A. and Sano T.; 2000: *Criteria for seismic microzoning of a large area in central Italy.* In: Proc. of 12th World Conf. of Eart. Eng., Auckland, Jan., 2000, CD-Rom.

Pratt T. L. and Brocher T. M.; 2006: *Site response and attenuation in the Puget Lowland, Washington state*. Bull. Seism. Soc. Am., **96**, 536-552.

Roded R.; 1996: *Geological map of Dimona, Geological Survey of Israel*. 1:50 000, Sheet 19-1.

Rozenbaum A.G., Zilberman E., Bar-Matthews M., Ayalon A. and Agnon A.; 2004*: Tufa deposits in Bet Shean Valley - mapping and facies descriptions.* GSI Report No ES-37, 51 pp.

Shapira A. and Avirav V.; 1995: *PS-SDA Operation Manual.* Technical Report IPRG, The Institute for Petroleum Research and Geophysics, Z1/567/79, 24 pp.

Shapira A., Avni R. and Nur A.; 1993: *A new estimate for the epicentre of the Jericho earthquake of 11 July 1927.* Isr. Journ. Earth Scien., **42**, 93-96.

Shapira A., Feldman L., Zaslavsky Y. and Malitzk, A.; 2001: *Application of a stochastic method for the development of earthquake damage scenarios: Eilat, Israel test case.* The Problems of Lithosphere Dynamics and Seismicity, Computational Seismology, **32**, 58-73.

Storn R. and Price K., 1995: *Differential evolution: A simple and efficient adaptive scheme for global optimization over continuous spaces.* Technical Report TR-95-012, International Computer Science Institute, Berkeley.

Theodulidis N., Bard P.Y., Archuleta R. and Bouchon M.; 1996: *Horizontal-to-vertical spectral ratio and geological conditions: the case of Garner valley downhole in Southern California.* Bull. Seism. Soc. Am., **68,** 767-779.

Toshinawa T., Taber J. J. and Berrill J. B; 1997: *Distribution of ground motion intensity inferred from questionnaire survey, earthquake recordings, and microtremor measurements- a case study in Christchurch, New Zealand, during 1994 Arthurs pass earthquake.* Bull. Seism. Soc. Am., **87**, 356-369.

Zaslavsky Y., Gitterman Y. and Shapira A., 1995: *Site response estimations using week motion measurements.* In: Proceedings of 5th Inter. Conf. on Seismic Zonation, Nice, France, Oct., pp. 1713-1722.

Zaslavsky Y., Shapira A. and Arzi A.A.; 2000: *Amplification effects from earthquakes and ambient noise in Dead Sea Fault (Israel).* Soil Dynamics and Earthquake Engineering, **20**, 187-207.

Zaslavsky Y., Shapira A. and Leonov J.; 2003: *Empirical evaluation of site effects by means of H/V spectral ratios at the locations of strong motion accelerometers in Israel.* J. Earth. Eng., **7,** 655-677.

Zaslavsky Y., Shapira A., Gorstein M., Aksinenko T., Kalmanovich M., Ataev G., Giller V., Perelman N., Livshits I., Giller D. and Dan H.; 2005: *Expected site amplifications in the coastal plane of Israel.* In: Proc. of Inter. Conf. of Earth. Eng. in the 21st Century (EE-21C), Skopje, Aug., 2005, CD-Rom.

Zaslavsky Y., Gorstein M., Aksinenko T., Kalmanovich M., Ataev G., Giller V., Da H., Giller D., Perelman N., Livshits I. and Shvartsburg A.; 2006: I*nterpretation of mocrotremor H/V ratio in multilayered media: a study at Haifa bay, Israel.* In: Proc. of First European Conf. on Earthquake Engineer. and Seism., Geneva, Sept., 2006, CD-Rom.

Zhao B., Horike M. and Takeuchi Y.: 2000: *Analytical study on reliability of seismic site-specific characteristics estimated from microtremor measurements.* In: Proc. of 12th World Conf. of Earth. Eng., Auckland, January, 2000, CD-Rom.

Corresponding author: Yuly Zaslavsky
Seismology Division, Geophysical Institute of Israel
P.O. Box 182, Lod, Israel.
phone: +972 8 9785846; fax: +972 8 9255211; e-mail: yuly@seis.mni.gov.il